International Journal of Nanoelectronics and Materials
Volume 16 (Special Issue) December 2023 [207-220]

Enhancement of Electrochemically Reduced Graphene Oxide (ErGO) UV Photo Detector Performance via Direct One-Step Electrode Deposition Technique

Norhazlin Khairudin[1], Muhammad Faiezzam Rahim[1], Mohammad Haziq Ilias[1], Norsyahirah Ramli[1], Muhammad Arman Abdul Manah[1], Rozina Abdul Rani[2], Maizatul Zolkapli[1], and Ahmad Sabirin Zoolfakar[1,*]

[1]School of Electrical Engineering, College of Engineering, Universiti Teknologi MARA, 40450, Shah Alam, Selangor, Malaysia
[2]School of Mechanical Engineering, College of Engineering, Universiti Teknologi MARA, 40450, Shah Alam, Selangor, Malaysia

ABSTRACT

Recently, photodetectors have garnered significant attention owing to their broad spectrum of applications across fields such as the biomedical, industrial, agricultural, and telecommunications sectors. This research focuses on the development of a UV photodetector based on electrochemically reduced graphene oxide (ErGO) and incorporates reduced graphene oxide (rGO) thin films on interdigitated Au electrodes. The rGO thin films were synthesized using the direct one-step deposition method, maintaining a constant water bath temperature of 40 °C, and a consistent GO concentration of 0.15 g, while varying the pH levels within the range of pH 8 to pH 10. The investigation primarily concentrated on assessing the surface morphological, structural, and electrical properties of the rGO thin films by altering the pH level when exposed to 365 nm ultraviolet (UV) irradiation. The significant parameters for evaluating photodetector performance, including photosensitivity, stability, repeatability, response time, and recovery time. To achieve this, advanced techniques such as field-emission scanning electron microscopy (FESEM), Raman spectroscopy, and current-time measurement are employed. As a finding, the fabricated UV PD of rGO-Au at pH 9 achieved the photosensitivity 96.5% with the stability that was 30 times greater than rGO-Au (pH 10) and superior repeatability as well as rapid switching rate as compared to pH 8 and pH 10 with 0.6 V bias. This implies that rGO-Au prepared at pH 9 is a suitable material for application in UV detection.

Keywords: Reduced Graphene Oxide (rGO), green route, direct one-step electrode deposition technique, UV Photodetector, photo response characteristic

1. INTRODUCTION

Photodetectors have recently garnered substantial attention in both fundamental research and industrial applications, finding widespread use in fields such as security [1], inter-space communications [2], military operations [3], biological imaging [4], and environmental monitoring [5]. A photodetector is a photoelectric device that converts electromagnetic radiation, carrying energy in the form of light, into an electrical signal, either as photocurrent or photovoltage [6]. Conventional photodetectors often rely on thicker materials to enhance their photoelectric response, but they suffer from several drawbacks, including fragility, high production costs, and the requirement for harsh manufacturing environments. These limitations significantly restrict their utility in flexible, transparent, and stretchable devices. In pursuit of more promising photodetector materials, various options have emerged, including metal oxides like SnO_2[7], ZnO [8], TiO_2 [9], In_2Te_3 [10], Bi_2O_3 [11] NiO [12], Sb_2Te_3 [13], Ga_2O_3 [14], and graphene derivatives.

* Corresponding authors: ahmad074@uitm.edu.my

Among these materials, graphene has gained significant attention for its potential in ultraviolet (UV) photodetector applications. Graphene, composed of a monolayer of sp2 hybridized carbon atoms arranged in a two-dimensional honeycomb lattice, has captured the scientific community's interest due to its exceptional electrical and thermal conductivity [15], structural integrity [16], mechanical strength [17], unique optical properties [18], extensive specific surface area [19], high carrier mobility [20], and chemical characteristics. It exhibits desirable attributes such as a tuneable work function, high carrier mobility, and excellent light transmission. However, its lack of a bandgap poses challenges for various applications, necessitating tailored modifications to unlock its full potential. To enhance graphene's applicability, numerous methods have been developed. The exfoliation of graphite stands as one of the most employed techniques for synthesizing graphene, resulting in graphene oxide (GO) that is hydrophilic and water-dispersible due to the presence of oxygen-containing groups (carboxyl, epoxy, carbonyl, and hydroxyl) [21][22][23][24]. To overcome the structural defects introduced by these groups, researchers have extensively explored methods for obtaining high- quality graphene that closely resembles pristine graphene.

One promising approach involves the chemical and thermal conversion of graphene oxide (GO) derived from natural graphite using the Hummers' method, offering advantages in terms of cost-effectiveness and scalability. However, chemical reduction methods often employ toxic reagents, such as hydrazine, dimethylhydrazine, metal hydride, and hydroquinone, posing risks to the environment [25], [26]. On the other hand, thermal reduction may present explosion hazards, and its kinetics and mechanisms are not fully understood, requiring cautious treatment of larger samples [27]. The high temperatures needed for oxygen group removal can be a complex process and costly [28]. The subsequent restoration process, encompassing the reduction of graphene oxide (GO) to yield reduced graphene oxide (rGO), is crucial as it significantly influences the resulting material's structure and quality [1]. Thus, researchers have explored the use of rGO instead of pristine graphene due to its adjustable surface defect density, enhanced sensitivity, and superior conductivity compared to graphene oxide (GO). The rGO exhibits a band gap ranging from 1.19 eV to 1.58 eV, rendering it an excellent candidate for mechanical, electrical, and optical devices application [29][9].

Among the various techniques, electrochemical deposition emerges as the most practical option, offering simplicity, environmental friendliness, and cost-effectiveness while avoiding the use of hazardous chemicals, with no toxic residues that could harm the ecosystem. This method effectively removes the oxygen functional groups (OFGs) in graphene oxide, yielding high- quality rGO structures resembling pristine graphene [30] [31].

Hence, the objective of this investigation is to assess varying pH levels during the electrodeposition process impact the performance of rGO-based UV photodetectors. The deposition of rGO was carried out on Au substrate using a direct one-step deposition method, encompassing a variation of pH conditions: pH 8, pH 9, and pH 10. The rGO deposition process was executed on Au interdigitated electrode, with a width spacing of 200 μm. The deposition procedure entailed a potential sweep ranging from -0.2 V (start-stop), with a vertex range spanning from -0.4 V (upper vertex) to -1.1 V (lower vertex), and a scan rate of 0.005 V/s. This cyclic process was repeated ten times for each sample, with the entire procedure being conducted within a water bath temperature of 40 °C. To comprehensively assess the sample characteristics and their suitability for UV detection, a collection of experimental apparatus was employed. To attained this, the investigation of surface morphology and structural properties was examined by Field Emission Scanning Electron Microscopy (FESEM) and Raman Spectroscopy, as well as the evaluation of their photo response towards UV irradiation in terms of sensitivity, stability, repeatability, response time, and recovery time via current-time measurements.

2. MATERIAL AND METHODS

2.1 Preparation of Graphene Oxide Solution

Three beakers were initially filled with a pH 7.4 Phosphate-Buffered Saline (PBS) solution provided by R&M Chemicals. To achieve specific pH levels of 8, 9, and 10, sodium hydroxide granules from Sigma-Aldrich were gradually introduced into each respective beaker. After successfully adjusting the pH, 0.15g of graphite powder (C, Aldrich 99%) was added to each PBS mixture, and the solutions were stirred using a magnetic stirrer for a period of 15 minutes.

2.2 Fabrication of rGO Via Direct One-Step Electrode Deposition Technique

The electrochemical process for depositing rGO involved the use of three standard electrodes: the working electrode (WE), counter electrode (CE), and reference electrode (RE). These electrodes were connected to three separate probes attached to the electrochemical deposition (ECD) system, as illustrated in Fig. 1(a)-(b). The materials employed as the Working Electrode (WE), Reference Electrode (RE), and Counter Electrode (CE), in the electrochemical deposition procedures for reduced graphene oxide (rGO) deposition were Gold (Au), Silver/Silver Chloride (Ag/AgCl) and Platinum (Pt) electrodes respectively. The substrate for the deposition of reduced graphene oxide (rGO) was an Au interdigitated electrode, has dimensions of 2.2 cm in length, 0.76 cm in width, 0.07 cm in thickness, and featured 200 µm width spacing, as illustrated in Figure 1 (c). The GO solution was poured into a titration glass, and all three electrodes were submerged in this GO solution. The titration glass, with the GO solution and electrodes, was then placed in a deionized (DI) water bath at 40 °C and allowed to equilibrate for a few minutes to reach the equilibrium temperature. Following this, cyclic voltammetry (CV) analysis was conducted using specific parameters, including a vertex ranging from -0.4 V to -1.1 V (upper and lower), 10 scan cycles, and a scan rate of 0.005 V/s. Each window was assessed at sweep potential -0.2 V (start-stop). During this process, rGO thin films were electrochemically deposited onto the Aurum electrode surface.

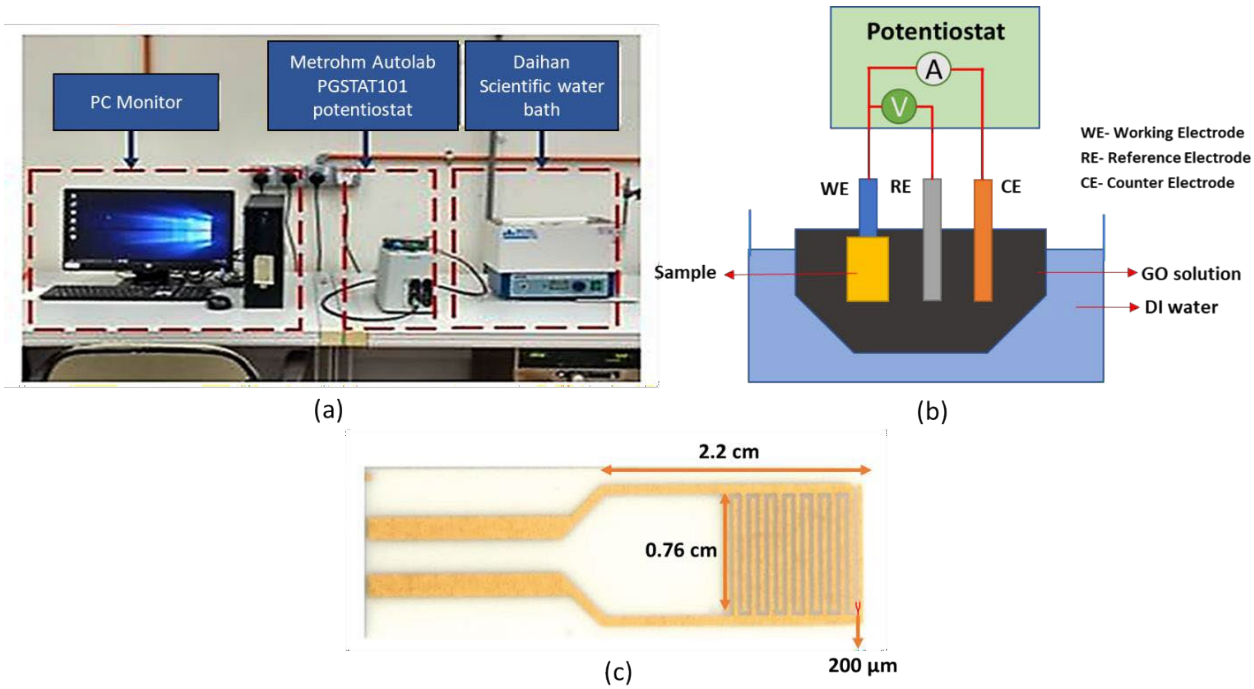

Figure 1. (a) The arrangement of apparatus for ECD process, (b) The schematic diagram of ECD method, (c) The sample top view Au interdigitated electrode dimensions.

2.3 Material and Electrical Characterization

The surface morphology of the deposited reduced graphene oxide (rGO) films was examined through Field Emission Scanning Electron Microscopy (FEI NOVA NANOSEM 230) at an acceleration voltage of 10 kV. FESEM analysis allowed for the acquisition of high-resolution surface details of the rGO thin films, revealing intricate nano structural features. Raman spectroscopy, employing the NTEGRA SPECTRA MT-MDT system, was employed to probe the material properties of the rGO thin films deposited on Au substrates. This involved irradiating the samples with a laser beam at a 432 nm wavelength, serving as the excitation source. Raman spectroscopy enabled an investigation of defects and alterations in the crystal structure of the material. Additionally, Raman spectroscopy facilitated the characterization of the photoelectric performance of the thin film deposited as pH levels varied. Furthermore, to assess the electrical properties of the rGO thin films, current versus time (I-t) measurements were conducted. A UV lamp, specifically the UVP UVGL-55 model 6 Watt, 0.16 Amps, 230V with 50-60Hz, emitting a 365 nm wavelength, was employed to illuminate the sample. The sensor measurement system, utilizing the Keithley 2400 Source Meter Unit (SMU) instrument, facilitated the evaluation of the photodetector's performance under both UV-illuminated and non-illuminated conditions. The experiments were carried out using different pH levels, encompassing 5 samples (n= 5) for each of pH 8, pH 9, and pH 10. The measurement involved employing ON-OFF switching intervals of 150 seconds for each pulse, allowing up to maximum of 5 cycles of illumination, an applied potential of 0.6 V. The resulting graph data was subsequently analyzed to assess parameters such as sensitivity, stability, response time, recovery time, and repeatability. Figure 2 exhibits the experimental set up for current-time measurement.

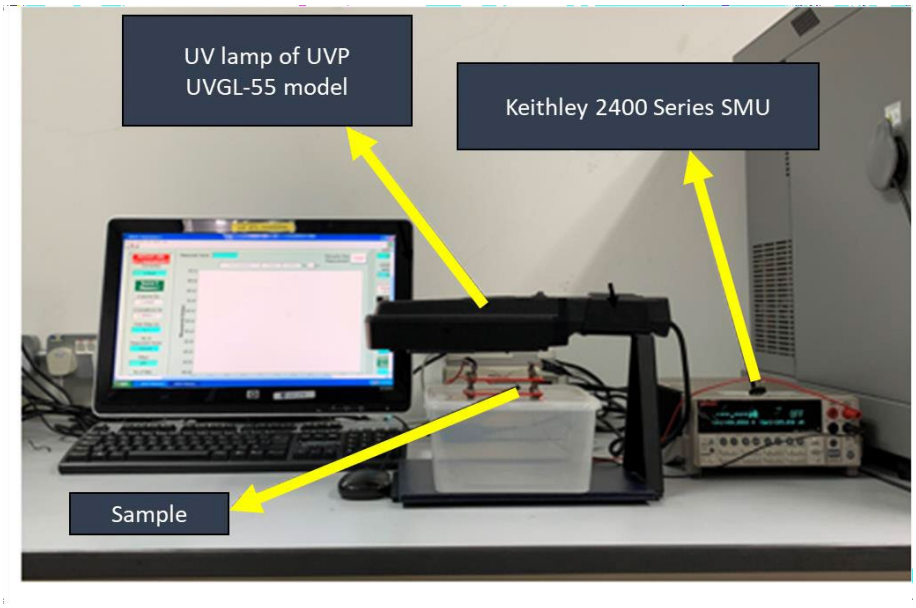

Figure 2. The experimental set-up for current versus time measurement.

3. RESULTS AND DISCUSSION

3.1 Material Properties

3.1.1 Field Emission Scanning Electron Microscopy (FESEM)

Figure 3 (a)-(c) provides a detailed examination of the surface morphology of the rGO thin films under varying pH conditions (pH 8, pH 9, and pH 10). This analysis was conducted using Field Emission Scanning Electron Microscopy (FEI NOVA NANOSEM 230) at an acceleration voltage of 10 kV. The morphology observed in the reduced graphene oxide (rGO) thin films revealed distinctive features, characterized by a wrinkled, wavy, non-uniform, and crumbled nanosheet structure. These observations are indicative of the transformation from graphene oxide (GO) to reduced graphene oxide (rGO).

Figure 3 (a) provides a clear illustration of the wrinkled, wavy, and irregular distribution of rGO at pH 8, showcasing the alterations in the material's morphology. This distinctive characteristic becomes particularly pronounced in the case of rGO at pH 10 represented in Figure 3 (c). It is notable that spherical clusters become intertwined within the rGO layers and exhibit a crumpled and agglomerated on rGO surface as the pH of the rGO increases. The pH elevation in the GO solution may induce a phase transition which promotes the growth of nanocrystal grains which agreed reported in literature [9], [17], [32].

However, as illustrated in Figure 3 (b), the rGO thin film demonstrates a layered, wavy, and uniformly distributed wrinkled surface at a pH of 9. The surface morphology results in increased surface area-to-volume ratio [33][17], a characteristic that can significantly increase the material's sensitivity to incident UV light, thus elevating its ability to capture UV photons and increasing the mobility of charge carriers within the rGO layers. Additionally, the presence of an evenly distributed wrinkled surface is contributing to improved light deflection, corresponding well with the findings reported in the literature [33][34][35].

Furthermore, it has the potential to improve its performance on sensitivity, speed, stability, and repeatability when applied in UV detection applications.

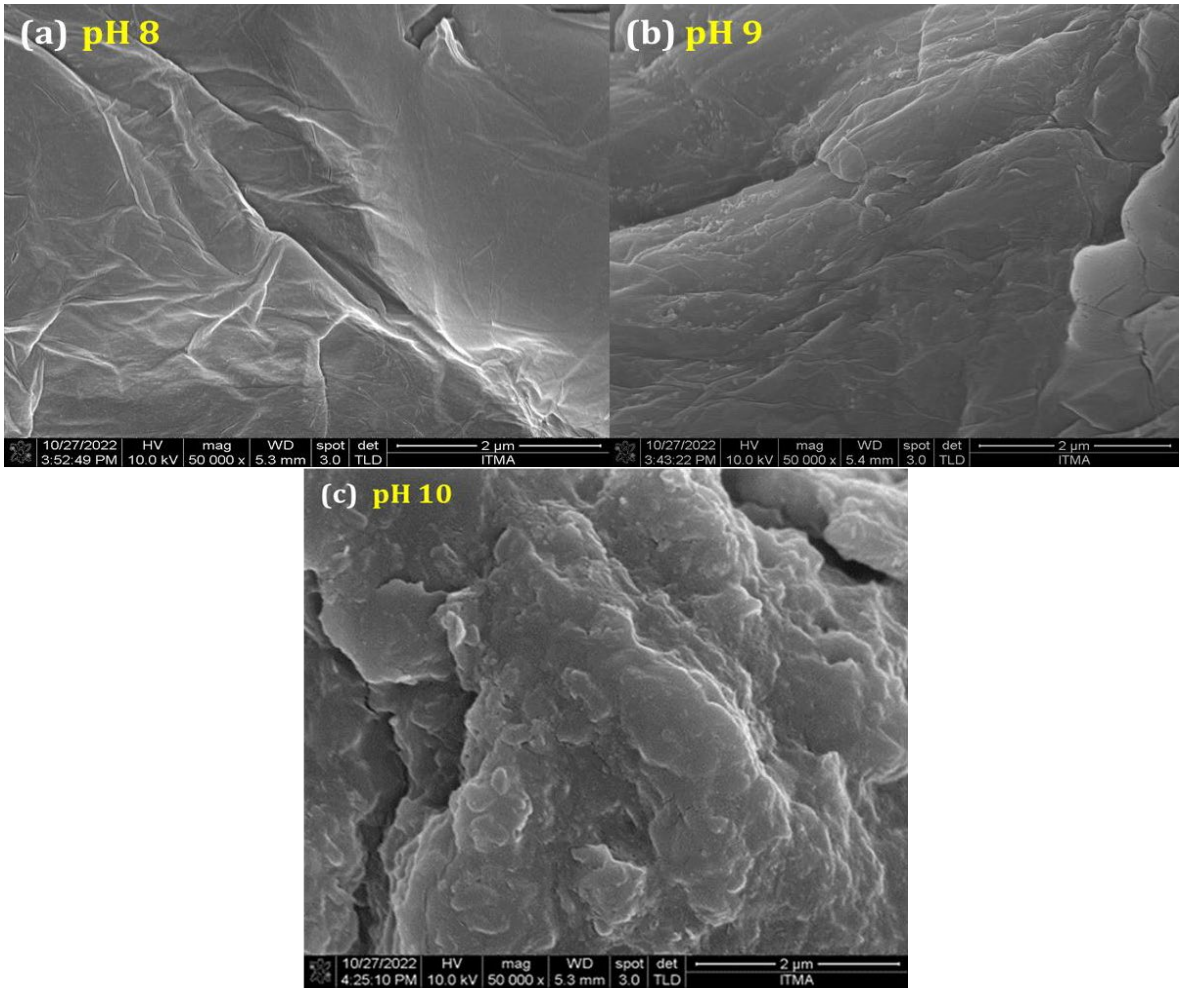

Figure 3. FESEM micrographs of rGO thin films as a function of variation of (a) pH 8 (b) pH 9 (c) pH 10.

3.1.2 RAMAN Spectroscopy

Raman spectroscopy was employed to investigate both defects and alterations in the crystal structure following the reduction process from graphene oxide (GO) to reduced graphene oxide (rGO). The Raman spectrum was used to assess the photoelectric performance of the rGO thin film under varying pH conditions (pH 8, pH 9 and pH 10). Figure 4 illustrates the prominent Raman peaks, specifically the D band and G band. The D band serves as an indicator of structural imperfections [36]–[38] within the crystal lattice of thin films made from reduced graphene oxide (rGO), while the G band corresponds to carbon-carbon (C-C) bonds of sp2 hybridized in the thin film material [30], [39]. The appearance of the G-band peak can be attributed to the vibrational mode of sp2 carbon atoms bonded within the plane [40], while the presence of structural imperfection hinders the D band due to out-of-plane vibrations. The notable D peak demonstrates a Raman shift observed at different values for rGO thin film at pH levels of 10, 9, and 8, specifically 1364 cm-1, 1359 cm-1 and 1357 cm-1 respectively. Conversely, the G band displayed a Raman shift at distinct values on the rGO thin film at the same pH levels, that is 1594 cm-1, 1591 cm-1 and 1590 cm-1. Furthermore, the relative peak intensity between band D and band G can be estimated to assess the degree of imperfection (defects) in the rGO crystal structure. According to Raman analysis, the relative intensity ratio of the D band to the G band (ID/IG) for rGO was determined to be 1.68, 1.66 and 1.71 on pH 10, pH 9 and pH 8 correspondingly. The findings indicate that as the pH of the GO solution increases, the ID/IG intensity ratio decreases, signifying the complete reduction of GO to rGO through the removal of oxygenated functional groups (OFGs) [22], [41]. According to the literature, graphene oxide (GO) typically exhibits an ID/IG ratio of

approximately 0.90 [9], [42], which is lower than the ID/IG ratio observed for reduced graphene oxide (rGO). The higher ID/IG indicates the imperfections in the crystal structure of rGO, likely arising from the formation of holes and voids in rGO networks during the reduction process as stated in[35][36]–[38], [43] . While there is a slight similarity in the structural defects within the pH range of 8 to 10, it is notable that pH 9 exhibits fewer structural imperfections compared to pH 8 and pH 10, as indicated by lower ID/IG ratio. This suggests that pH 9 provides better structural, good conductivity, and lessens recombination effects which the factors may lead to enhance UV photodetection performance.

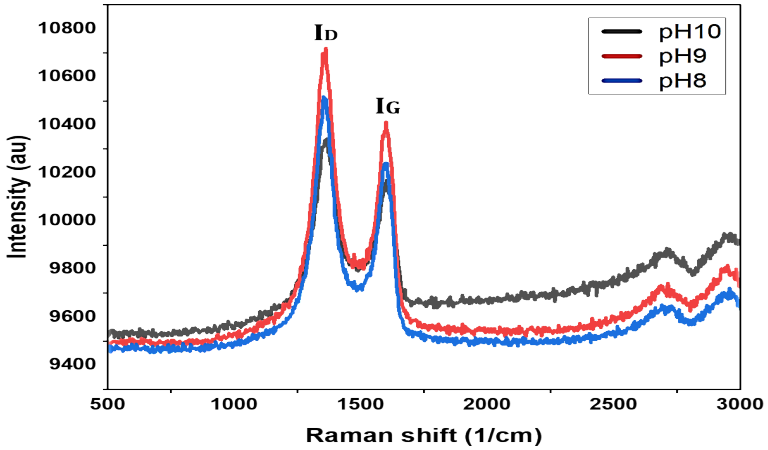

Figure 4. Raman spectra in relation to pH variation.

3.2 Electrical Properties

The evaluation of photodetector performance is determined by analyzing the current-time relationship. The sample was subjected to characterization across varying pH levels (pH 8, pH 9, and pH 10). This characterization comprised five cycles of alternating UV illumination at a wavelength of 365 nm and non-UV illumination, at 0.6 V potential. The performance parameters for the rGO samples encompass sensitivity, stability, response time, recovery time, and repeatability. Figure 5 illustrates the current-time curve of the rGO UV photodetector in relation to pH. The sample's performance can be calculated using equations 1 and equation 2.

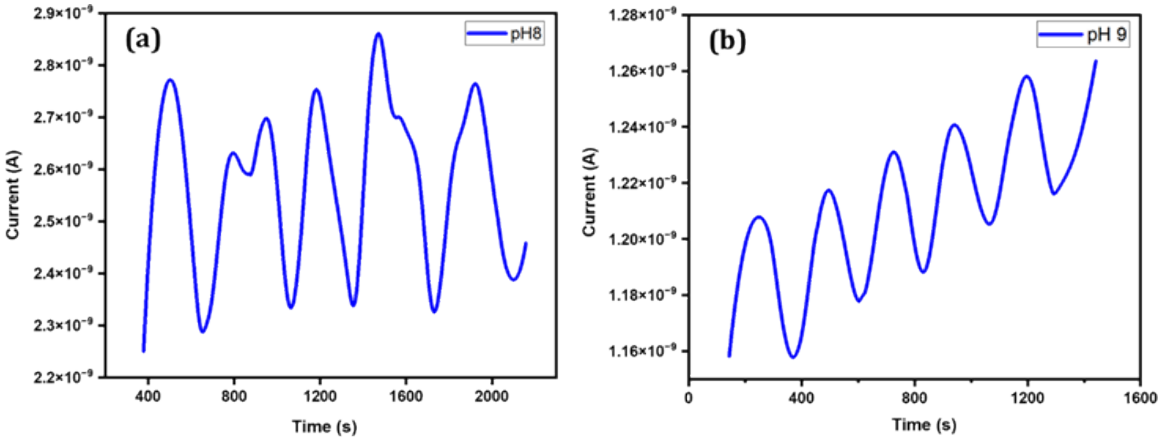

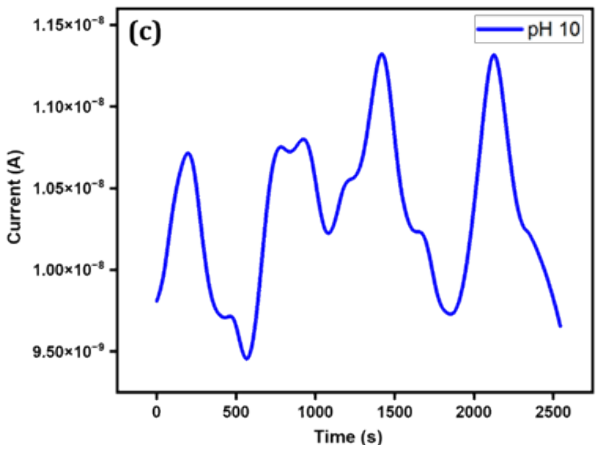

Figure 5. The repeatability in the transition between UV ON/OFF states of photodetectors based on rGO thin films, operated at a 0.6 V bias voltage and exposed to 365 nm UV light, with variations in pH (a) pH 8, (b) pH 9, and (c) pH 10.

The current-time reactions of the rGO-Au photodetector, with an applied potential of 0.6 V, were recorded for sensitivity assessment, as depicted in Figure 5. To compute the sensitivity to UV light based on these graphs, the following equation (1)[33] is employed:

$$S = \frac{I_{photo}}{I_{dark}} \times 100\ \% \quad (1)$$

In equation 1, I photo denotes the differences current between I light measured in the presence UV illumination while I dark represents the dark current observed when light is absent.

The assessment of sample stability can be conducted by analyzing fluctuations in the photocurrent response. The minimal deviation seen in the sample suggests enhanced stability. The stability can be quantified using the equation (2) [33] as follows:

$$Stability = \sum_0^5 \frac{I_{light}}{no\ of\ cycles} - \sum_0^5 \frac{I_{dark}}{no\ of\ cycles} \quad (2)$$

Figures 5 (a)-(c) depict current-time measurements acquired from the rGO-Au thin film with a 200 µm spacing, maintained at a potential of 0.6 V, and subjected to UV illumination at a wavelength of 365 nm. These measurements aimed to investigate the film's response under varying pH conditions, specifically pH 8, pH 9, and pH 10, as well as its response in the absence of UV illumination. The outcomes revealed a gradual increase in photocurrent generation at pH 9 when exposed to ultraviolet (UV) radiation. The p-type behavior of rGO is characterized by a Fermi level (EF) energy of 4.6 eV [44], [45], notably lower than that of Au, which falls within the range 5.10 eV to 5.47 eV. The surface of the rGO thin film absorbs phonon energy, which has the potential to excite electrons from the valence band to the conduction band within the rGO layers.

The resulting holes, generated in the valence band, were swept away in the opposite direction by the electric field that induced through Schottky contact [46]. The mechanism leads to the formation of electron-hole pairs (EHPs), ultimately resulting in photocurrent generation. Additionally, the hot carriers within the conduction band of the rGO layers can traverse into the metal Au electrode, thereby enhancing the overall charge carrier within the rGO-Au system, particularly at pH 9. It is reasonable to conclude that the pH 9 rGO photodetector demonstrates remarkable photodetection capabilities under 365 nm UV light illumination, primarily due to its higher phonon absorption [10], [47], [48].

Moreover, the rGO sample prepared with pH 8 and pH 10, where there is a noticeable deviation in photocurrent generation under both UV illumination and non-illumination over five cycles. The variability in photocurrent generation at these pH levels indicates that neither pH 8 nor pH 10 is conducive to achieving satisfactory photocurrent production compared to pH 9. Furthermore, it exhibits a higher degree of repeatability in the switching behavior of photocurrent, as evident from the I-t curves observed throughout five cycles at pH 9. The photocurrent consistently rises to a peak upon exposure to UV at 365 nm and diminishes rapidly when UV light is absent. Table 1 highlights the stability, with values of 0.042 x 10-9 A, 0.428 x 10-9 A, 1.264 x 10-9 A, recorded at pH 9, pH 8 and pH 10, respectively, under a 0.6 V bias. Remarkably, the photocurrent generated at pH 9 remains stable during both illumination and non-illumination intervals, as proved by the stability values.

Table 1 Electrical parameters of rGO-Au UV PD for different pH of GO solution at 0.6 V biased

Sample	Sensitivity (%)	Stability (x 10^{-9} A)	Response Time (s)	Recovery Time (s)
pH 8	81.71	0.428	87.5	93
pH 9	96.5	0.042	68	57
pH 10	87.02	1.264	84	171

In contrast, rGO at pH 9 reveals the highest sensitivity, reaching a remarkable 96.5% in its ability to detect UV light, surpassing the performance of rGO at pH 8 and pH 10, which achieved sensitivities of 81.71% and 87.02%, respectively. Additionally, it demonstrates faster response and rapid recovery times when exposed to UV light. Notably, the faster recovery time at pH 9 indicates a small occurrence of recombination, in contrast to the longer recombination time of 171 s observed at pH 10 [11], [13], [49].

This can be ascribed to the recombination process involving electrons trapped within voids states, arising from structural imperfection within the crystal, in the absence of UV light. This alignment with the findings reported by [49] and further clarified by Raman analysis. Furthermore, the built-in electric field formation at the rGO-Au film interface, accelerating charge carrier separation and limiting the recombination process, may result in reduced dark current and faster response at pH 9. The lower dark current (I dark=1.1 x 10-9 A) observed in rGO-Au at pH 9 may be attributed by its improved crystalline structure in comparison to the irregular and crumpled structure that was identified by FESEM analysis at pH 10 (I dark=9.8 x 10- 9 A) as reported in [50].

Moreover, it is evident that the rGO-Au film at pH 9 exhibits greater sensitivity in UV detection, approximately fifth fold and double fold higher than the MgxZn1-xO films and heterostructure ZnO-(Ga, Ag)-ZnO nanorods of UV PDs that achieved using magnetron sputtering and cost-effective two-step process method respectively as recorded in Table 2 of a previously published UV PD sensor study.

Table 2 Comparison of sensitivity between the fabricated work and the recently reported UV Photodetector

Structure Material	Fabrication method	Sensitivity (%)	Response/Recovery time (s)	Bias (V)	Ref.
MgZnO (42.8 at%)	Magnetron sputtering	20	-	9V	[15]
Psi only	Modified polyol method	24.69	0.8/0.15	5V	[51]
ZnO/ (Ga, Ag)-ZnO nanorod	Cost-effective two-step process	40	13/18	1V-5V	[2]
Ag - ZnO	Hydrothermal	32.9	-	5V	[33]
rGO-Au	Direct One-step deposition technique	96.5	68/57	0.6V	This work

As evident from the data, the rGO-Au UV sensor proposed at pH 9 demonstrates superior sensitivity compared to previously developed UV photodetectors. Consequently, the observed enhancements in sensitivity, stability, response time, recovery time, and repeatability at pH 9 make it an appealing material for future development in fabricating high-performance UV photodetectors.

3.3 UV Photo Detector Mechanism

As the UV rays illuminate the rGO thin film sampled, some of incident photon absorbed in rGO layer. The incident photon's absorption induces the transition of an electron from the valence band to the conduction band within the layers of rGO, resulting in the generation of electron- hole pairs (EHP). This process leads to the accumulation of electrons on the surface of sampled [2], [33], [52]. This generated EHP was mobile and travel within the rGO material. The presence of these mobile charge carriers within the rGO layer causes an alteration in the material's conductivity. Electrons in the conduction band follow a path to the metal through the Schottky barrier, resulting in the generation of a photocurrent [12], [17], [53].

Notably, the work function of rGO (ϕ rGO) exhibited greater than (ϕ Au), facilitating the passage of photoexcited electrons from the rGO layer's conduction band through the metal electrode, thereby contributing to the photocurrent [54], [55]. Concurrently, the holes, created in the valence band of the reduced graphene oxide (rGO), exhibit the capability to drift in varying directions within the rGO layers or undergo transport to the rGO-metal interface in response to the electric field [56].

The recombination process between these holes and injected electrons within the metal electrodes can give rise to the emission of radiant light, potentially amplifying the magnitude of the electric current traversing the device [34], [57], [58]. Conversely, in the absence of UV illumination, there is a reduction in the generation of electron-hole pairs, leading to a decrease in the flow of electrical current within the photodetector. Figure 6 illustrates the energy band diagram of rGO-Au when exposed to UV illumination at a wavelength of 365 nm.

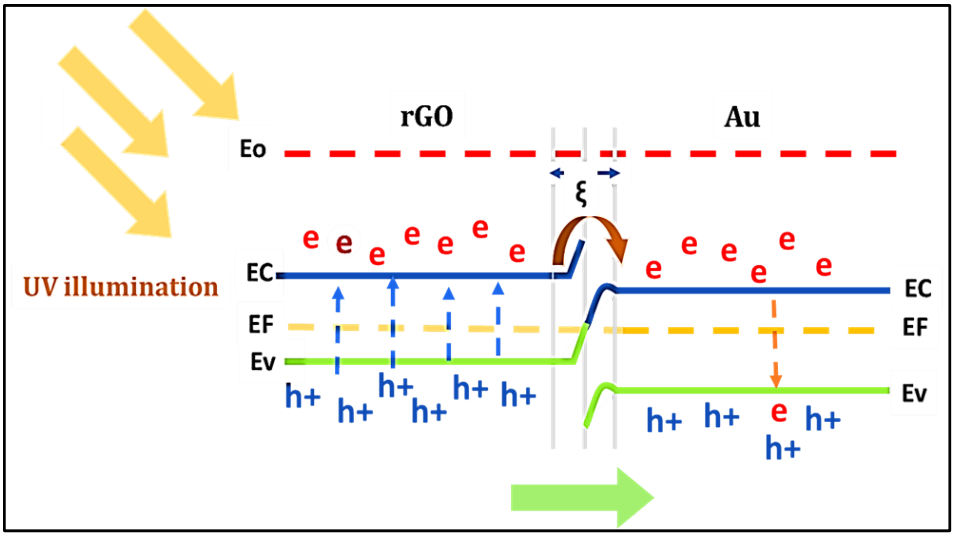

Figure 6. The energy band diagram of rGO-Au under UV illumination.

4. CONCLUSION

In summary, we reported the successful synthesis of rGO-Au UV photodetectors employing a sustainable, straightforward, and cost-effective direct one-step electrodeposition (ECD) technique, with pH variation employed for sample characterization. Our investigation reaches into the surface morphology of the synthesized samples, revealing a distinct layered and wavy structure of rGO uniformly deposited onto the Au substrate. This unique morphology, which facilitates efficient light transmission along a well-defined propagation path, is supported by Raman analysis indicating a lower occurrence of defects in the crystal structure of rGO-Au at pH 9. This reduction in defects is expected to contribute to a decrease in recombination losses and an increase in photocurrent generation. The performance of these UV photodetectors is assessed, with a notable UV photo response of 96.5% achieved at a specific wavelength of 365 nm. This remarkable enhancement, representing a five-fold improvement over MgxZn1-xO films and a doubling of performance compared to heterostructure ZnO- (Ga, Ag)-ZnO nanorods UV photodetectors fabricated using magnetron sputtering and a cost-effective two-step process, respectively, underscores the potential of our synthesized rGO-Au photodetectors. Among the various pH conditions studied, rGO-Au at pH 9 emerges as the standout candidate, showcasing superior sensitivity, stability, repeatability, as well as faster response and recovery times. These findings highlight the promising prospects of this material structure for applications in the field of UV detection.

ACKNOWLEDGMENTS

This work is supported under an internal grant of Universiti Teknologi MARA known as Geran Penyelidikan Khas 600-RMC/GPK 5/3 (091/2020).

REFERENCES

[1] Ahmed, A. Singh, S. J. Young, V. Gupta, M. Singh, & S. Arya, "Synthesis techniques and advances in sensing applications of reduced graphene oxide (rGO) Composites: A review," Compos. Part A Appl. Sci. Manuf., vol. 165 (2023) pp. 107373.

[2] GuruSampath Kumar, X. Li, Y. Du, Y. Geng, & X. Hong, "UV-photodetector based on heterostructured ZnO/(Ga,Ag)-co-doped ZnO nanorods by cost-effective two-step process," Appl. Surf. Sci., vol. 509 (2020) pp. 144770.

[3] H. Kumar & M. C. S. Kumar, "Sensors and Actuators A : Physical Indium sulfide based metal-semiconductor-metal ultraviolet-visible photodetector," Sensors Actuators, A, vol. 299 (2019) pp. 111643–111654.

[4] S. Safa, S. Mokhtari, A. Khayatian, & R. Azimirad, "Improving ultraviolet photodetection of ZnO nanorods by Cr doped ZnO encapsulation process," Opt. Commun., vol. 413 (2017) pp. 131–135.

[5] Y. Liu *et al*., "Self-powered solar-blind deep-UV photodetector based on CuI/Ga2O3 heterojunction with high sensitivity," Sensors Actuators A Phys., vol. 349 (2023) pp. 1–7.

[6] P. Phukan & P. P. Sahu, "High performance UV photodetector based on metal-semiconductor-metal structure using TiO2-rGO composite," Opt. Mater. (Amst)., vol. 109 (2020).

[7] W. Tian, H. Lu, & L. Li, "Nanoscale ultraviolet photodetectors based on onedimensional metal oxide nanostructures," Nano Res., vol. 8 (2015) pp. 382–405.

[8] M. A. Khan, A. Kumar, J. Zhang, & M. Kumar, "Recent advances and prospects in reduced graphene oxide-based photodetectors," J. Mater. Chem. C., vol. 9 (2021) pp. 8129-8157.

[9] A. S. AlShammari, M. M. Halim, F. K. Yam, & N. H. M. Kaus, "Effect of precursor concentration on the performance of UV photodetector using TiO2/reduced graphene oxide (rGO) nanocomposite," Results Phys., vol. 19 (2020) p. 103630.

[10] H. Figiel, O. Zogał, & V. Yartys, "Recent advances in one-dimensional electrospun semiconductor nanostructures for UV photodetector applications: A review," J. Alloys Compd., vol. 404–406 (2023) p. 169718.

[11] S. Ren *et al*., "Rational design and large-scale synthesis of convex Bi2O3 nanospheres for self-powered UV imaging photodetector," Mater. Sci. Semicond. Process., vol. 165 (2023) p. 107689.

[12] M. Jia, F. Wang, L. Tang, J. Xiang, K. S. Teng, & S. P. Lau, "High-Performance Deep Ultraviolet Photodetector Based on NiO/β-Ga2O3 Heterojunction," Nanoscale Res. Lett., vol. 15 (2020).

[13] S. K. Chetia, A. K. Das, R. S. Ajimsha, R. Singh, P. S Padhi, & P. Misra, "Al2O3 barrier layer for enhancing UV to visible rejection ratio in p-Si/n-MgZnO heterojunction visible blind UV photodetectors," Phys. B Condens. Matter, vol. 663 (2023) p. 415021.

[14] R. K. D, Y. K, V. P, S. Muthusamy, & S. Bharatan, "Modeling and simulation of Ga2O3 thin film solar blind UV photodetector," Mater. Today Proc., (2023).

[15] J. S. Shiau, S. Brahma, J. L. Huang, & C. P. Liu, "Fabrication of flexible UV-B photodetectors made of MgxZn1-xO films on PI substrate for enhanced sensitivity by piezophototronic effect," Appl. Mater. Today, vol. 20 (2020) pp. 1–10.

[16] Chen, S. Zhang, B. Hu, H. San, Z. Cheng, & W. Hofmann, "Non-aligned ZnO nanowires composited with reduced graphene oxide and single-walled carbon nanotubes for highly responsive UV–visible photodetectors," Compos. Part B Eng., vol. 164 (2019) pp. 640–647.

[17] N. Khairudin *et al*., "Enhancing Humidity Performance: Effect of Electrode Material on Electrochemical Reduced Graphene Oxide (ERGO) Humidity Sensor," Int. J. Integr. Eng., vol. 14 (2022) pp. 215–228.

[18] A. Ngqalakwezi, D. Nkazi, G. Seifert, & T. Ntho, "Effects of reduction of graphene oxide on the hydrogen storage capacities of metal graphene nanocomposite," vol. 358 (2020) pp. 338-344.

[19] H. Kalita, V. S. Palaparthy, M. S. Baghini, & M. Aslam, "To appear in: Carbon," vol. 165 (2020) pp 9-17.

[20] H. Sun, G. Lu, H. Lv, & Z. Liu, "Graphene-supported silver nanoparticles for pH-neutral electrocatalytic oxygen reduction," Proc. IEEE Conf. Nanotechnol., (2013) pp. 598–601.
[21] M. J. Yoo & H. B. Park, "Effect of hydrogen peroxide on properties of graphene oxide in Hummers method," vol. 141 (2018) pp. 515-522.
[22] S. Wu, Z. Yin, Q. He, X. Huang, X. Zhou, & H. Zhang, "Electrochemical Deposition of Semiconductor Oxides on Reduced Graphene Oxide-Based Flexible, Transparent, and Conductive Electrodes," J. Phys. Chem., vol. 114 (June 2010) pp. 11816–11821.
[23] M. H. Ilias, R. A. Rani, & M. Z. Ahmad, "Effect of interdigital electrode material on the performance of an electrochemically Reduced Graphene Oxide chemiresistive humidity sensor," 2021 IEEE Reg. Symp. Micro Nanoelectron., (2021) pp. 133–136.
[24] N. Khairudin *et al*., "Effect of IDE Spacing on the Performance of ErGO Chemiresistive Humidity Sensor," Proc. - 2021 IEEE Reg. Symp. Micro Nanoelectron. RSM 2021, (2021) pp. 108–111.
[25] J. Aixart, F. Díaz, J. Llorca, & J. Rosell-Llompart, "Increasing reaction time in Hummers' method towards well exfoliated graphene oxide of low oxidation degree," Ceram. Int., vol. 47 (2021) pp. 22130–22137.
[26] H. Omar *et al*., "A review of synthesis graphene oxide from natural carbon based coconut waste by Hummer's method," Mater. Today Proc., vol. 75 (2023) pp. 188–192.
[27] G. A. Viana, D. S. da Silva, R. Landers, J. N. de Freitas, M. G. Villalva, & F. das Chagas Marques, "Desorption of chemical species during thermal reduction of graphene oxide films," Surf. Coatings Technol., vol. 463 (2023) p. 129524.
[28] M. A. H. Mohd *et al*., "Study of the Effect of Temperature on Humidity Sensing Properties of Electrochemical Reduced Graphene Oxide (ERGO)," IEEE Int. Conf. Semicond. Electron. Proceedings, ICSE, (2020) pp. 108–111.
[29] N. Sharma, M. Arif, S. Monga, M. Shkir, Y. K. Mishra, & A. Singh, "Investigation of bandgap alteration in graphene oxide with different reduction routes," vol. 513 (2020) p. 145396.
[30] Aksoy & D. Anakli, "Synthesis of Graphene Oxide Through Ultrasonic Assisted Electrochemical Exfoliation," Open Chem., vol. 17 (2019) pp. 581–586.
[31] A. Zhou, J. Bai, W. Hong, & H. Bai, "Electrochemically reduced graphene oxide: Preparation, composites, and applications," Carbon N. Y., vol. 191 (2022) pp. 301–332.
[32] P. K. Singh, K. Sharma, & P. K. Singh, "A low cost, bulk synthesis of the thermally reduced graphene oxide in an aqueous solution of sulphuric acid & hydrogen peroxide via electrochemical method," Inorg. Chem. Commun., vol. 140 (2022) p. 109378.
[33] S. Rajamanickam, S. M. Mohammad, I. A. Razak, A. Muhammad, & S. M. Abed, "Enhanced sensitivity from Ag micro-flakes encapsulated Ag-doped ZnO nanorods-based UV photodetector," Mater. Res. Bull., vol. 161 (2023) p. 112148.
[34] P. Phukan & P. P. Sahu, "High performance UV photodetector based on metal-semiconductor-metal structure using TiO2/rGO composite," Opt. Mater. (Amst)., vol. 109 (2020) p. 110330.
[35] Wang, H. Zhang, F. Yang, Y. Fan, & Q. Liu, "Enhanced light scattering effect of wrinkled transparent conductive ITO thin film," RSC Adv., vol. 7 (2017) pp. 25483–25487.
[36] Z. Li, L. Deng, I. A. Kinloch, & R. J. Young, "Raman spectroscopy of carbon materials and their composites: Graphene, nanotubes and fibres," Prog. Mater. Sci., vol. 135 (2020).
[37] V. Natarajan, M. Ahmad, J. Paul Sharma, A. Sathya, P. Kumar Sharma, & R. Thangaraj, "Interfacial charge-transfer for robust Raman quenching in staggered band aligned n-SnS2/p-rGO heterostructures," Appl. Surf. Sci., vol. 550 (2021) p. 149356.
[38] S. Nongthombam, N. Aruna Devi, S. Sinha, W. Ishwarchand Singh, & B. P. Swain, "Analysis of structural defects with the chemical composition of rGO/GaN nanocomposites using Raman spectroscopy," Mater. Today Proc., vol. 74 (2023) pp. 744– 749.
[39] M. Coros *et al*., "Green synthesis, characterization and potential application of reduced graphene oxide," Phys. E, vol. 119 (2020) p. 113971.
[40] M.-S. Chae, T. H. Lee, K. R. Son, H. Park, S. Hwang, & T. G. Kim, "Electrochemically metal-doped reduced graphene oxide films: Properties and applications," J. Mater. Sci. Technol., vol. 40 (2020) pp. 72–80.

[41] Karačić *et al*., "Electrochemical reduction of thin graphene-oxide films in aqueous solutions – Restoration of conductivity," Electrochim. Acta, vol. 410 (2022) p. 140046.
[42] N. Kumar & V. C. Srivastava, "Simple Synthesis of Large Graphene Oxide Sheets via Electrochemical Method Coupled with Oxidation Process," ACS Omega, vol. 3 (2018) pp. 10233–10242.
[43] A. Y. Lee *et al*., "Raman study of D* band in graphene oxide and its correlation with reduction," Appl. Surf. Sci., vol. 536 (2021) p. 147990.
[44] J. S. D. Rodriguez *et al*., "Modulating chemical composition and work function of suspended reduced graphene oxide membranes through electrochemical reduction," Carbon N. Y., vol. 185 (2021) pp. 410–418.
[45] M. Minella, F. Sordello, & C. Minero, "Photocatalytic process in TiO2/graphene hybrid materials. Evidence of charge separation by electron transfer from reduced graphene oxide to TiO2," Catal. Today, vol. 281 (2017) pp. 29–37.
[46] N. S. Khairir *et al*., "Schottky behavior of reduced graphene oxide at various operating temperatures," Surfaces and Interfaces, vol. 6 (2017) pp. 229–236.
[47] P. V. K. Yadav, B. Ajitha, Y. A. Kumar Reddy, & A. Sreedhar, "Recent advances in development of nanostructured photodetectors from ultraviolet to infrared region: A review," Chemosphere, vol. 279 (2021) p. 130473.
[48] A. S. AlShammari, M. M. Halim, F. K. Yam, K. M. Chahrour, M. E. Raypah, & N. H. M. Kaus, "The effect of spray cycles on the morphological, structural, and optical properties of rGO thin film deposited using spray pyrolysis technique," Mater. Sci. Semicond. Process., vol. 127 (2021) p. 105655.
[49] M. Abiyyu *et al*., "Ambient Processed rGO / Ti 3 CNT x MXene Thin Film with High Oxidation Stability, Photosensitivity, and Self-Cleaning Potential," vol. 15 (2023) pp. 44075-44086.
[50] S. Mondal, S. Ghosh, & D. Basak, "Extraordinarily high ultraviolet photodetection by defect tuned phosphorus doped ZnO thin film on flexible substrate," Mater. Res. Bull., vol. 144 (2021) p. 111490.
[51] A, A. M. Alqanoo, N. M. Ahmed, M. R. Hashim, M. A. Almessiere, S. A. Taya, & S. H. Zyoud, "Silver nanowires assisted porous silicon for high photodetector sensitivity using surface plasmonic phenomena," Sensors Actuators A Phys., vol. 347 (2022) p. 113942.
[52] A. Pandit, E. F. Schubert, & J. Cho, "Dual-functional ultraviolet photodetector with graphene electrodes on AlGaN/GaN heterostructure," Sci. Rep., vol. 10 (2020) p. 22059.
[53] N. S. Khairir, M. R. M. Hussin, I. M. Nasir, A. S. M. M. Uz-Zaman, W. F. H. Abdullah, & A. Sabirin Zoolfakar, "Study of Reduced Graphene Oxide for Trench Schottky Diode," IOP Conf. Ser. Mater. Sci. Eng., vol. 99 (2015).
[54] Ferrari *et al*., "Understanding the nature of graphene oxide functional groups by modulation of the electrochemical reduction: A combined experimental and theoretical approach," Carbon N. Y., vol. 203 (2023) pp. 29–38.
[55] Z. Ye *et al*., "Enhanced UV photo-detection properties of graphene oxide incorporated transparent TiO2 thin films in Schottky configuration," Appl. Geochemistry, vol. 49 (2023) pp. 20651-20661.
[56] Z. Lv *et al*., "A High Responsivity and Photosensitivity Self-Powered UV Photodetector Constructed by the CuZnS/Ga2O3 Heterojunction," Adv. Mater. Interfaces, vol. 10 (2023).
[57] P. V. Karthik Yadav, B. Ajitha, Y. A. K. Reddy, V. R. Minnam Reddy, M. Reddeppa, & M. D. Kim, "Effect of sputter pressure on UV photodetector performance of WO3 thin films," Appl. Surf. Sci., vol. 536 (2021) p. 147947.
[58] R. Ranjan, M. Kumar, & A. S. K. Sinha, "CdS supported on electrochemically reduced rGO for photo reduction of water to hydrogen," Int. J. Hydrogen Energy, vol. 44 (2019) pp. 10573–10584.